Body Temperature-Related Structural Transitions of Monotremal and Human Hemoglobin

I. Digel, Ch. Maggakis-Kelemen, K. F. Zerlin, Pt. Linder, N. Kasischke, P. Kayser, D. Porst, A. Temiz Artmann, and G. M. Artmann
Department of Cellular Engineering, University of Applied Sciences Aachen, 52428 Juelich, Germany

ABSTRACT In this study, temperature-related structural changes were investigated in human, duck-billed platypus (*Ornithorhynchus anatinus*, body temperature $T_b = 31–33°C$), and echidna (*Tachyglossus aculeatus*, body temperature $T_b = 32–33°C$) hemoglobin using circular dichroism spectroscopy and dynamic light scattering. The average hydrodynamic radius (R_h) and fractional (normalized) change in the ellipticity (F_{obs}) at 222 ± 2 nm of hemoglobin were measured. The temperature was varied stepwise from 25°C to 45°C. The existence of a structural transition of human hemoglobin at the critical temperature T_c between 36–37°C was previously shown by micropipette aspiration experiments, viscosimetry, and circular dichroism spectroscopy. Based on light-scattering measurements, this study proves the onset of molecular aggregation at T_c. In two different monotremal hemoglobins (echidna and platypus), the critical transition temperatures were found between 32–33°C, which are close to the species' body temperature T_b. The data suggest that the correlation of the structural transition's critical temperature T_c and the species' body temperature T_b is not mere coincidence but, instead, is a more widespread structural phenomenon possibly including many other proteins.

INTRODUCTION

Structural transitions of the hemoglobin (Hb) molecule induced by oxygen binding are well known and have been extensively characterized (1–4), and the thermal denaturation of hemoglobin has recently gained great interest (5). Previous studies have shown that a number of human hemoglobin variants denatured thermally more readily than did human HbA (6,7). Studies on denaturation of hemoglobins as a function of temperature, using optical rotatory dispersion and two-dimensional infrared correlation spectroscopy (8–12), have revealed a two-staged thermal transition mechanism of denaturation. Nevertheless, these and other studies (13) on denaturation of hemoglobins do not mention any transition events occurring around body temperature. At the initial structural perturbation stage (30–44°C), only the fast red shift of the band from an α-helix has been found, indicating that the native helical structures become more solvent exposed as temperature increases.

Artmann et al. (14) reported a critical temperature of $T_c = 36.4°C \pm 0.3°C$ for human red blood cells (RBCs) at which they undergo a sudden phase transition-like change in their mechanical properties. This was observed in micropipette experiments for erythrocytes changing from blocking to passing through 1.3 ± 0.2-μm micropipettes, when applying 2.3-kPa aspiration pressure (14).

Nonmonotonous slopes of the Arrhenius plots obtained later in Hb viscosimetry studies (15) suggested that the cellular phenomenon was linked to hemoglobin. An obvious finding was the extremely high activation energy (366.6 kJ/mol) within the temperature range of 35–38°C for concentrated hemoglobin solutions (50 g/dL) compared to 55.1–58.1 kJ/mol found for higher and lower temperatures, respectively. Such nonlinear behavior is in general believed to be related to protein phase transitions (16). Remarkably, the changes in viscosity appeared at the same temperature range as a transition found later with circular dichroism (CD) spectroscopy using purified oxygenated and deoxygenated hemoglobin solutions (17).

These studies provoked further methodological and theoretical questions about the physiological and biophysical mechanisms involved in the hemoglobin temperature transition phenomenon. The fact that the temperature transition of human Hb was observed at normal body temperature could be coincidence or, to the contrary, linked to the physiological temperature of a particular species. Investigation of hemoglobins from different species with different body temperatures could help elucidate this issue.

This study reports comparative measurements of temperature-dependent changes in the hydrodynamic radius and structure for human (*Homo sapiens*), monotremal echidna (*Tachyglossus aculeatus*), and platypus (*Ornithorhynchus anatinus*) hemoglobins—chosen for their distinctly different body temperatures (~32–33°C for both species) compared to humans (37°C). Two questions were posed in this study: 1), can hemoglobin temperature transitions be seen in static and dynamic light scattering (DLS) experiments, and 2), is there any correlation between the species' body temperature, T_b, and the structural transition temperature, T_c?

CD spectroscopy was used to study the overall structural organization of hemoglobin (18–20). Although the CD signal could show an aggregation- and size-related scattering effect,

Submitted May 2, 2006, and accepted for publication July 3, 2006.

Address reprint requests to Dr. Ilya Digel, Laboratory of Cell Biophysics Aachen, University of Applied Sciences, Ginsterweg, 1, D-52428 Jülich, Germany. E-mail: digel@fh-aachen.de.

0006-3495/06/10/3014/08 $2.00
doi: 10.1529/biophysj.106.087809

light scattering allows more precise detection of protein particle size. Thus analyzing the fluctuation of scattered light could provide valuable information on the hydrodynamic radius (R_h), which may rapidly change at T_c. A comparison of the hydrodynamic radii of hemoglobin molecules at different temperatures could provide information regarding unfolding and hydration characteristics of the proteins.

MATERIALS AND METHODS

Blood samples

Human venous blood (2 mL) was obtained from healthy adult donors and collected into heparinized syringes. Venous blood from free-living adult echidnas (*T. aculeatus*) and platypuses (*O. anatinus*) were used as monotreme blood; ~2 mL of heparinized blood was obtained from each animal and maintained at 2°C until analyzed.

Sample preparation

Air-oxygenated Hb was used in all experiments. Oxy-Hb samples were prepared from erythrocyte (RBCs) suspensions obtained from whole blood (17). RBCs were harvested by centrifugation at 2000 × *g* for 10 min. RBCs (0.5 mL) of the pellet were added to 9.5 mL CD buffer solution (0.1 M KCl, 61.3 mM K_2HPO_4, 5.33 mM KH_2PO_4) (21) and washed three times at 4200 × *g* for 10 min. If necessary, the pH (7.4) and osmolarity (290–300 mOsm) were adjusted with KH_2PO_4. RBCs (0.4 mL) were then hemolyzed in 3.6 mL distilled water, and 1 mL of this solution was added to 9 mL CD buffer, filtered, separated by column electrophoresis, and diluted further with CD buffer. Since absolute ellipticities in CD spectroscopy are concentration dependent, the final Hb concentrations of 0.1–0.75 mg/mL were used for both CD and light-scattering measurements. The hemoglobin concentration was determined spectrophotometrically using a millimolar extinction coefficient of 13.5 at 541 nm for oxyhemoglobin (22). Additionally, the samples were analyzed by conventional sodium dodecyl sulfate-polyacrylamide gel electrophoresis (SDS-PAGE) for purity.

Circular dichroism measurements

Far-ultraviolet (UV) CD spectra were measured with a Jasco J720 CD spectropolarimeter (Jasco, Tokyo, Japan) equipped with a temperature Peltier controller. Thermal unfolding of hemoglobin was studied between 25°C and 45°C in a 0.1-cm-thick quartz cuvette with a 0.1-cm optical path length (Hellma, Jena, Germany).

Comparison of the actual temperature inside the cuvette with the temperature set by the Peltier element showed a deviation <0.1°C for this temperature interval. The starting temperature of the hemoglobin solution was adjusted to 25°C and then (stepwise or gradually) increased. In the case of stepwise temperature increments, the temperature was set manually and the sample was allowed to equilibrate for 1 min at each temperature point. For gradual temperature increase, a temperature ramp was set to 0.1°C min^{-1}.

Subsequently, a complete wavelength scan (wavelength steps 1 nm, average time = 4 s, time response = 2 s, band width = 1 nm) was carried out in the far-UV region between 190 and 260 nm. This procedure was repeated three times, with a new sample each time. Temperature scans of pure buffer solutions were carried out at identical conditions to those used for hemoglobin solutions. Blank spectra were subtracted from the Hb spectra at each temperature point. From these wavelength scans, the absolute and relative ellipticities at 222 ± 2 nm were derived, representing a measure of the α-helical content of the proteins. This wavelength was chosen since the CD method is most sensitive at 222 nm to α-chain content in globins (23). The fractional (normalized) change in the observed ellipticity at 222 ± 2 nm was calculated according to (9)

$$F_{obs} = [E_{obs}(T) - E_{max}]/[E_{25} - E_{max}],$$

where $E_{obs}(T)$ is the ellipticity at 222 nm at temperature T, E_{max} is the ellipticity at the maximum temperature (°C) used, and E_{25} is the ellipticity at 25°C. The same normalizing algorithm was applied for evaluations of the light-scattering data.

Dynamic light-scattering measurements

DLS data were obtained with a temperature-controlled DAWN-EOS instrument equipped with quasielastic light-scattering module (Wyatt Technology, Santa Barbara, CA) in a temperature range of 25–45°C. The sample temperature was changed (stepwise or gradually) as described above for CD measurements. Temperature variations during a single measurement never exceeded ±0.2°C.

The instrument was used in batch (not flow-through) mode using glass scintillation cells filled bubble-free with a 4-mL sample. Hb samples were filtered twice through Millipore (Bedford, MA) 0.2-μm pore size filters and degassed in vacuum, when necessary. The time-dependent autocorrelation function (ACF) of the photon current was monitored with a software correlator provided by the manufacturer. The first sampling time was 0.96 μs. ACFs were taken and sampled every 2 s, containing 10^5–10^6 counts each. Sets of ACFs collected at corresponding temperatures were averaged and stored for analysis. Light-scattering data analysis was performed using a second-order cumulant function (24):

$$G(t_l) \leftarrow bl\{1 + sn|\exp(-\Gamma_1 t_l + \tfrac{1}{2}\Gamma_2 t_l^2)|^2\},$$

where Γ_1 and Γ_2 are the first and second cumulants, bl is the baseline in arbitrary counts, and sn is a parameter related to the signal/noise ratio (i.e., the maximum initial value of the correlation function). The following formula relates the hydrodynamic radius R_h to the first cumulant, Γ_1:

$$R_h = k_B T q^2/6\pi\eta\Gamma_1 \quad \text{where} \quad q^2 = (4\pi n_s/\lambda_0)sin(\Theta/2),$$

where λ_0 is the vacuum wavelength of incident light, n_s is the index of refraction of the solution, Θ is the scattering angle, k_B is the Boltzmann constant, and η is the solvent viscosity at the experimental Kelvin temperature T. The sample polydispersity was computed from $P = \Gamma_2/(\Gamma_1)^2$. This quantity was used for discarding data that showed values of $p > 0.05$, indicating excessive noise due to aggregates or dust. In the computation, the value of R_h was normalized to CD buffer. Similarly, the radius was corrected for the refractive index, assuming $n = 1.329$ for water at 783 nm.

Statistical treatment of experimental data

For statistical analysis, all experiments were repeated multiple times. Common statistical procedures (standard deviation, Student's *t*-tests) were applied to the data using Microsoft Excel 2003 package (Unterschleissheim, Germany). In the case of highly scattered values, the Epanechnikov smoothing kernel was applied using LabView Software (National Instruments, (Austin, TX) as well as SPSS Software (SPSS, Munich, Germany). Unless stated otherwise, standard deviation is shown in the figures.

RESULTS

Thermal denaturation of hemoglobins was monitored between 190 and 260 nm at stepwise, increased temperatures between 25°C and 45°C. As expected, the far-UV CD spectra of Hb purified from RBCs contained a typical α-helical signature, with local minima at 208 and 222 nm (25). The minimum at 222 nm was selected to monitor the temperature-dependent changes in ellipticity.

Fig. 1 illustrates the phenomenon of nonlinearity of thermal unfolding for monotremal and human hemoglobins at physiological temperatures. The accelerated loss in ellipticity, beginning between 33°C and 35°C, is clearly visible. The denaturation curves are uneven and have characteristic S-shapes for all studied hemoglobins that can be interpreted as ''slow-fast-slow rate'' in terms of unfolding speed. Thus, for each examined hemoglobin type, there is a temperature interval where significant structural changes are induced by slight temperature changes.

To determine the structural transition temperature for each species with higher precision, the obtained S-curves were divided into three quasilinear parts—each approximated by a linear function. The cross sections of the best-fitting lines were regarded as the beginning and end of the accelerated transition temperature interval (T_c). This interval is shown in Fig. 1 and corresponds to molecular rearrangements which have been referred to as ''structural transition''.

The transition was always observed at the same temperature for a given hemoglobin type in a given solvent. For human hemoglobin, the transition was found to occur in the range from 36°C to 37°C, in agreement with previous data (17). The monotremal hemoglobins demonstrated principally a similar characteristic. However, the structural transition was observed at a lower temperature range (33–35°C for both species).

CD is sensitive to structural changes of proteins as well as to light scattering (26–27). Thus, the temperature transition observed by CD spectroscopy has two possible causes: I), partial thermal unfolding of hemoglobin α- (HBA) helices, and II), changes in aggregation and/or in molecular size and shape. These processes were further investigated by DLS. In this method, the diffusion coefficient is correlated with protein size according to the Einstein-Stokes equation.

The heterogeneous particle size in Hb solutions is potentially problematic as Hb dissociates in diluted solutions into

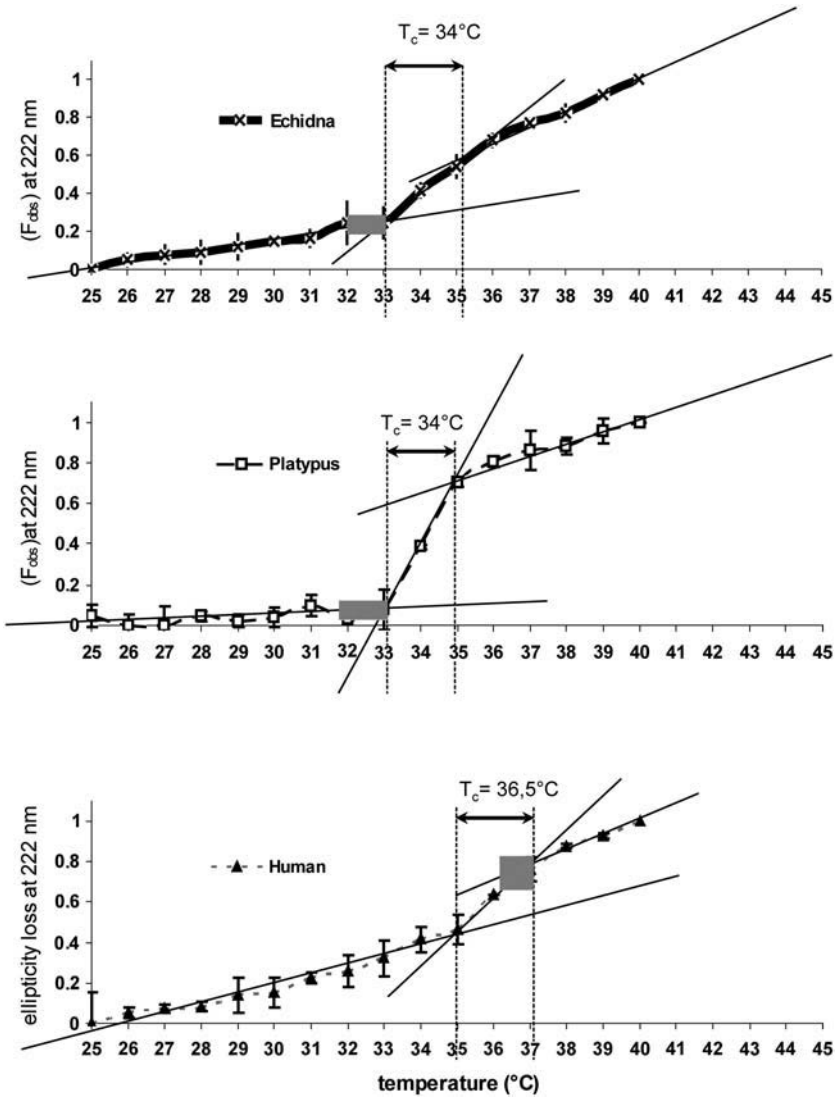

FIGURE 1 Fractional change in ellipticity at 222 ± 2 nm (F_{obs}) with temperature for oxyhemoglobins obtained from human blood and monotreme blood. Data points were averaged from the original CD data obtained from three to four samples of each type of hemoglobin. The error bars represent standard deviation of the respective fractional changes. Straight lines show approximation of three distinctly linear parts of the graph. Temperature intervals where the transition occurs are marked as T_c (critical temperature) for each species. Gray boxes show physiological temperature range for each species.

dimers and monomers, but not without the appearance of large intermolecular aggregates. The resulting particles significantly differ in size and shape; as a result, the scattering signal is noisy and must be processed further using smoothing algorithms. Fig. 2 shows a typical original data plot of a light-scattering experiment before and after mathematical data processing. As seen in the CD experiments, the nonlinearity of size change with temperature is clearly observed, with a sharp turning point (''kink'') found for each hemoglobin type almost exactly at the critical temperature, as seen previously.

Multiple temperature scans at identical conditions were undertaken as countermeasures against high data dispersion. The normalized data collected from four light-scattering experiments for each animal sample are shown in Fig. 3. Unlike the S-shaped curves with two ''kinks'' obtained in CD measurements, DLS curves were found to be L-shaped. As with the CD data, almost linear regions can be defined on the curves, separated by a transition point which is visible as a kink in the curve. Comparison of the data from Figs. 1 and 3 strongly indicates that the structural transition of hemoglobins at T_c is always linked to body temperature, T_B, of a particular species.

According to computations based on the assumption of the quasispherical shape of hemoglobin molecules, the values of R_h were consistent among $R_h = 3.15$–3.20 nm (average $R_h =$ 3.17 nm). These values are in accordance with those reported previously for hemoglobin (24). The consistently increasing radius of hemoglobins with rising temperature may be attributed to the appearance of larger aggregates resulting from a slightly enhanced surface hydrophobicity and most likely not to a slight modification of the hydrodynamic shape due to partial unfolding.

The observed differences in temperature behavior for human and monotremes were obviously linked to the protein structure. All sequences shown in Fig. 4 were obtained from the SwissProt protein sequence database. The HBA sequences (with accession number) were P69905 human, P01979 platypus, P01977 and P01978 echidna; the hemoglobin β (HBB) sequences were P68871 human, P02111 platypus, P02110 echidna. Amino acid sequence alignments were determined according to the method developed previously by Myers and Miller (28). We also used a structure genetic matrix based on the work of Feng et al. (29). Multiple amino acid sequence alignments were made with the ''Clustal'' program (30–31).

Hemoglobins of the represented species were found to retain a remarkable degree of homology, with some sequences almost identical in both monotremal species. Overall comparison of the amino acid sequences of HBA and HBB subunits of human and monotremes resulted in 68.08% and 74.6% identities and 17.7% and 11.6% similarities (replacements with physicochemically similar amino acids), respectively. Owing to this remarkable evolutionary conservation of hemoglobin sequences, only 13–14% of the amino acid residues (19–20 amino acid residues per HBA or HBB chain) differ in their physicochemical properties.

Nevertheless, the comparative amino acid compositions of these hemoglobins show characteristic differences. Most notably, the number of nonpolar (hydrophobic) (Leu, Gly, Pro,

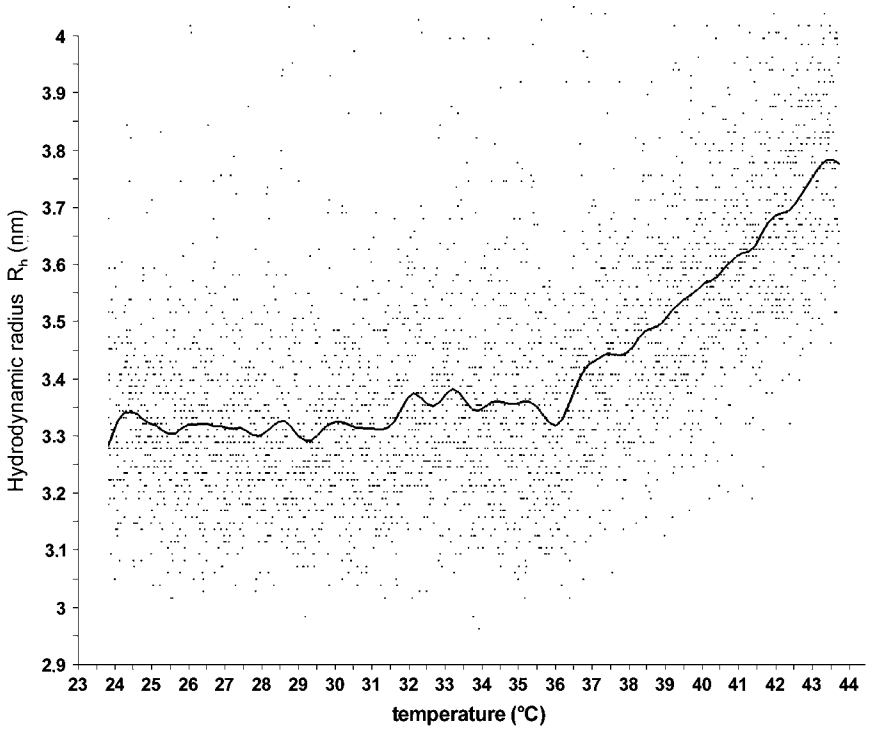

FIGURE 2 Original DLS data obtained for human hemoglobin (*dots*) and the resulting smoothing curve calculated by Epanechnikov kernel (*line*). A distinct kink is visible at ~36°C, representing the onset of accelerated particle size increase.

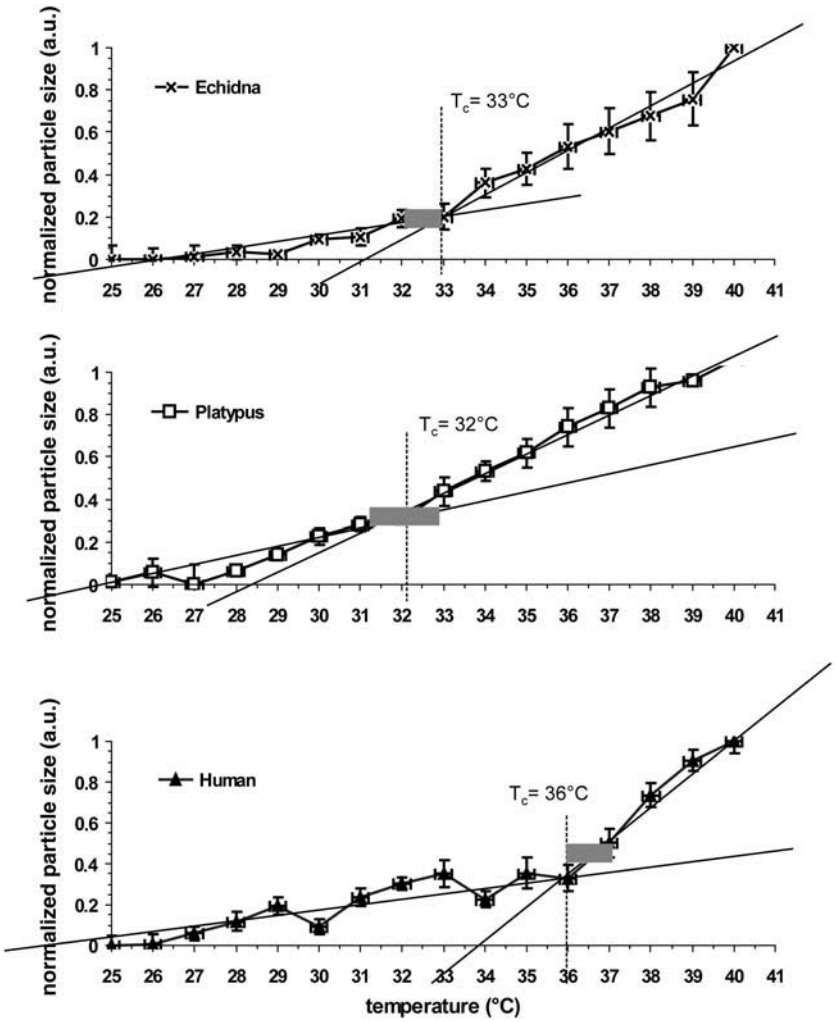

FIGURE 3 Fractional change of particle size with temperature for oxyhemoglobin solutions derived from DLS data. Data points were averaged from the original data obtained from three to four solutions of each type of hemoglobin. The error bars represent the standard deviation of the respective fractional changes. Straight lines show best approximation ($R^2 \rightarrow 1$) of two distinctly linear parts of the obtained L-shaped curves. The transition temperature interval may be defined as located close to the intersection point of best-approximating trend lines and is marked as T_c (critical temperature) for each species. Gray boxes show physiological body temperature range for each species.

Ala) amino acid residues is much higher in human Hb, accompanied by cluster-like substitutions between polar and charged amino acids in the middle of both α- and β-chains.

DISCUSSION

Protein thermal unfolding with subsequent aggregation plays a crucial role in protein science and medical engineering. Despite its biological importance, little is known about the mechanisms and potential pathways involved in the formation of molecular aggregates (12). Thermal aggregation of proteins is usually characterized by an irreversible two-state model (26,32) with the occurrence of folding/unfolding and intermediate or uncooperative events (33–37). The change of random coils appears at lower temperatures than those of all other secondary structure elements. At the thermal unfolding stage, the unfolding of solvent-exposed helical structures is claimed to guide the structural transitions (12). The temperature range 30–44°C has been generally described as an initial perturbation stage, without mentioning any peculiar temperature transition points. However, the DLS studies presented here have provided further evidence of the presence of a specific Hb temperature transition point first reported by Artmann (14) as a hemoglobin unfolding/aggregation event. As a reaction on temperature change, the tertiary structure of the protein became abruptly looser and several protein sites became more solvent exposed. The solvent-exposed structures are expected to be responsible for the onset of aggregation. At further thermal aggregation stages, the transition is dominated by the formation of aggregates and unfolding of the buried structures.

The important consequence of the study is that the effect is not restricted to human beings and could be of general physiological interest. A physiological meaning of the temperature transition of monotremes and human hemoglobins may be related to alterations in water balance. The protein hydration issue is of special interest, because the amount of nonsolvent water in Hb depends markedly on the temperature (38). It is important to note that the interaction of hemoglobin with water takes place in a ''crowded'' cytosolic environment, where water is scarce and activity is limited (24). The crucial role of molecular water bridges between hemoglobin molecules in

FIGURE 4 Amino acid sequence alignments of human, platypus, and echidna (minor α-chain marked as echidna-m) HBA and HBB sequences (28) (SwissProt Database). Additionally, a structure genetic matrix was used (29). Asterisks indicate identical residues, dots indicate similar residues, and exclamation marks indicate nonsimilar residues. The gray parts indicate ''hot spots'' in the Hb molecule where most substitutions take place.

high concentrated human hemoglobin solutions (45 g/dl) was discussed in a previous study where we reported a sudden viscosity drop around human body temperature (15). Preliminary estimations made by the same authors (15) indicate that the structural transition of Hb leads to partial release of hydration water in the range of decagrams per kilograms of body weight. The particular mechanisms of such temperature-induced dehydration are still to be revealed. The authors (15) also suggested that conformational changes of Hb molecules result in a thinning of the hydration shell. The data obtained now in CD and DLS studies rather support another hypothesis attributing the release of water to aggregation events. The assumed mechanism is that slight conformational rearrangements (CD data), when a protein undergoes a change in topology, seemingly favor self-association (DLS data) followed by releasing excessive water. In other words, partial unfolding with subsequent formation of larger protein aggregates could inevitably influence the protein hydration shell and the number of particles, resulting in a release of excess cell water into the bulk volume. This, in turn, would change the colloid-osmotic pressure balance between cytosol and blood plasma, potentially playing a role in homeostasis at fever conditions and hyperthermia (39–41).

The fact that the structural transition point is related with species' physiological core body temperature might have general biological relevance in respect to body temperature sensing and management. Based on knowledge about the pathophysiology of thermoregulation and heatstroke, one can hypothesize that changes in protein conformation induced by elevated temperature could play a role in triggering pathways responsible for thermal regulation. We would like to mention in this context a previous finding on a heat-induced microtubule protein disassembly shown to be highly correlated to species' body temperatures in mouse, rat, calf, and chicken (42). Interestingly the microtubule disassembly temperatures were within the range of fever temperatures of corresponding species.

There is also evidence of a relationship between protein conformation, normal body temperature, and lethal temperature of cells in culture. The maximum temperature of survival for chick fibroblasts (normal body temperature 42°C) was 46.5°C and for gonadal cells from rainbow trout (normal body temperature 12°C) was 26°C, respectively. It is thus conceivable that protein organization could serve as thermomediator(s) which modulate and/or initiate heat responses. These results are relevant to elevated temperature effects a), on cell shape (43); b), in reducing the ability of treated cells to interact with other cells, or cultured substrates (44); and c), in restricting the mobility of cell surface components (45). These and other studies also suggest that many proteins may play an important role in determining cellular functions in an elevated temperature environment. Turi et al. (41) suggested that proteins are active, functional units in the reception and transduction of environmental stimuli via stimulus-specific conformational changes. Thus, we hypothesize that this feature may be imprinted in the hemoglobin structure. In other words, nature knows by protein structure where body temperature must be set. Whether there exists a structural motive and how it makes body temperature unique must still be explored.

If this hypothesis proves to be true, further studies using hemoglobin from animals with a variety of different body temperatures could show a similar trend, leading to the conclusion that body temperature is imprinted into the structure of some proteins.

These experiments were partly performed at the Research Centre in Jülich in collaboration with Dr. Wolfgang Hüttel and Silke Bode. We thank Dr. Ira Tremmel for patience and perseverance in securing valuable monotremal blood samples for the experiments. We also thank Professor Gerhard Dikta (Aachen University of Applied Sciences) for help and suggestions regarding the mathematical analysis.

This work was supported by a grant to G. M. Artmann by the Ministerium für Innovation, Wissenschaft, Forschung und Technologie North Rhine Westphalia, Germany, and by the Center of Competence in Bioengineering at the Aachen University of Applied Sciences.

REFERENCES

1. Bettati, S., A. Mozzarelli, and M. F. Perutz. 1998. Allosteric mechanism of haemoglobin: rupture of salt-bridges raises the oxygen affinity of the T-structure. *J. Mol. Biol.* 281:581–585.
2. Knapp, J. E., M. A. Oliveira, Q. Xie, S. R. Ernst, A. F. Riggs, and M. L. Hackert. 1999. The structural and functional analysis of the hemoglobin D component from chicken. *J. Biol. Chem.* 274:6411–6420.
3. Levantino, M., A. Cupane, and L. Zimanyi. 2003. Quaternary structure dependence of kinetic hole burning and conformational substates interconversion in hemoglobin. *Biochemistry.* 42:4499–4505.
4. Lukin, J. A., G. Kontaxis, V. Simplaceanu, Y. Yuan, A. Bax, and C. Ho. 2003. Quaternary structure of hemoglobin in solution. *Proc. Natl. Acad. Sci. USA.* 100:517–520.
5. Bischof, J. C., and X. He. 2006. Thermal stability of proteins. *Ann. N. Y. Acad. Sci.* 1066:12–33.
6. Ruckpaul, K., H. Rein, and F. Jung. 1971. Correlations between thermal stability and circular dichroism of hemoglobin derivatives of different species. *FEBS Lett.* 13:193–194.
7. Clementi, M. E., S. G. Condo, M. Castagnola, and B. Giardina. 1994. Hemoglobin function under extreme life conditions. *Eur. J. Biochem.* 223:309–317.
8. Kinderlerer, J., H. Lehmann, and K. F. Tipton. 1970. Thermal denaturation of human haemoglobins. *Biochem. J.* 119:66P–67P.
9. Kinderlerer, J., H. Lehmann, and K. F. Tipton. 1973. The thermal denaturation of human oxyhaemoglobins A, A2, C and S. *Biochem. J.* 135:805–814.
10. Yang, T., and K. W. Olsen. 1988. Effects of crosslinking on the thermal stability of hemoglobins. II. The stabilization of met-, cyanomet-, and carbonmonoxyhemoglobins A and S with bis(3,5-dibromosalicyl) fumarate. *Arch. Biochem. Biophys.* 261:283–290.
11. Yang, T., and K. W. Olsen. 1990. The thermal stability of Hb O-Indonesia. *Hemoglobin.* 14:641–646.
12. Yan, Y. B., Q. Wang, H. W. He, and H. M. Zhou. 2004. Protein thermal aggregation involves distinct regions: sequential events in the heat-induced unfolding and aggregation of hemoglobin. *Biophys. J.* 86:1682–1690.
13. Sun, W. Q. 2000. Dielectric relaxation of water and water-plasticized biomolecules in relation to cellular water organization, cytoplasmic viscosity, and desiccation tolerance in recalcitrant seed tissues. *Plant Physiol.* 124:1203–1216.
14. Artmann, G. M., C. Kelemen, D. Porst, G. Buldt, and S. Chien. 1998. Temperature transitions of protein properties in human red blood cells. *Biophys. J.* 75:3179–3183.
15. Kelemen, C., S. Chien, and G. M. Artmann. 2001. Temperature transition of human hemoglobin at body temperature: effects of calcium. *Biophys. J.* 80:2622–2630.
16. Glaser, R. 2004. Biophysics. Springer, Berlin/Heidelberg/New York.
17. Artmann, G. M., L. Burns, J. M. Canaves, A. Temiz-Artmann, G. W. Schmid-Schonbein, S. Chien, and C. Maggakis-Kelemen. 2004. Circular dichroism spectra of human hemoglobin reveal a reversible structural transition at body temperature. *Eur. Biophys. J.* 33:490–496.
18. Chang, C. T., C. S. Wu, and J. T. Yang. 1978. Circular dichroic analysis of protein conformation: inclusion of the beta-turns. *Anal. Biochem.* 91:13–31.
19. Bierzynski, A. 2001. Methods of peptide conformation studies. *Acta Biochim. Pol.* 48:1091–1099.
20. Geraci, G., and L. J. Parkhurst. 1981. Circular dichroism spectra of hemoglobins. *Methods Enzymol.* 76:262–275.
21. Cameron, I. L., V. A. Ord, and G. D. Fullerton. 1988. Water of hydration in the intra- and extra-cellular environment of human erythrocytes. *Biochem. Cell Biol.* 66:1186–1199.
22. Antonini, E., and M. Brunori. 1970. Hemoglobin. *Annu. Rev. Biochem.* 39:977–1042.
23. Greenfield, N. J. 1996. Methods to estimate the conformation of proteins and polypeptides from circular dichroism data. *Anal. Biochem.* 235:1–10.
24. Arosio, D., H. E. Kwansa, H. Gering, G. Piszczek, and E. Bucci. 2002. Static and dynamic light scattering approach to the hydration of hemoglobin and its supertetramers in the presence of osmolites. *Biopolymers.* 63:1–11.
25. Li, R., Y. Nagai, and M. Nagai. 2000. Changes of tyrosine and tryptophan residues in human hemoglobin by oxygen binding: near- and far-UV circular dichroism of isolated chains and recombined hemoglobin. *J. Inorg. Biochem.* 82:93–101.
26. Dong, A., T. W. Randolph, and J. F. Carpenter. 2000. Entrapping intermediates of thermal aggregation in alpha-helical proteins with low concentration of guanidine hydrochloride. *J. Biol. Chem.* 275:27689–27693.
27. Bustamante, C., I. Tinoco Jr., and M. F. Maestre. 1983. Circular differential scattering can be an important part of the circular dichroism of macromolecules. *Proc. Natl. Acad. Sci. USA.* 80:3568–3572.
28. Myers, E. W., and W. Miller. 1988. Optimal alignments in linear space. *Comput. Appl. Biosci.* 4:11–17.
29. Feng, D. F., M. S. Johnson, and R. F. Doolittle. 1984. Aligning amino acid sequences: comparison of commonly used methods. *J. Mol. Evol.* 21:112–125.
30. Higgins, D. G., and P. M. Sharp. 1988. CLUSTAL: a package for performing multiple sequence alignment on a microcomputer. *Gene.* 73:237–244.
31. Higgins, D. G., and P. M. Sharp. 1989. Fast and sensitive multiple sequence alignments on a microcomputer. *Comput. Appl. Biosci.* 5: 151–153.
32. Lyubarev, A. E., B. I. Kurganov, V. N. Orlov, and H. M. Zhou. 1999. Two-state irreversible thermal denaturation of muscle creatine kinase. *Biophys. Chem.* 79:199–204.
33. Bulone, D., V. Martorana, and P. L. San Biagio. 2001. Effects of intermediates on aggregation of native bovine serum albumin. *Biophys. Chem.* 91:61–69.
34. Filosa, A., Y. Wang, A. A. Ismail, and A. M. English. 2001. Two-dimensional infrared correlation spectroscopy as a probe of sequential events in the thermal unfolding of cytochromes *c*. *Biochemistry.* 40: 8256–8263.
35. Paquet, M. J., M. Laviolette, M. Pezolet, and M. Auger. 2001. Two-dimensional infrared correlation spectroscopy study of the aggregation of cytochrome *c* in the presence of dimyristoylphosphatidylglycerol. *Biophys. J.* 81:305–312.
36. Yan, Y. B., R. Q. Zhang, and H. M. Zhou. 2002. Biphasic reductive unfolding of ribonuclease A is temperature dependent. *Eur. J. Biochem.* 269:5314–5322.
37. Yan, Y. B., Q. Wang, H. W. He, X. Y. Hu, R. Q. Zhang, and H. M. Zhou. 2003. Two-dimensional infrared correlation spectroscopy study of sequential events in the heat-induced unfolding and aggregation process of myoglobin. *Biophys. J.* 85:1959–1967.
38. Bobo, C. M. 1967. Nonsolvent water in human erythrocytes and hemoglobin solutions. *J. Gen. Physiol.* 50:2547–2564.
39. Ryan, M., and M. M. Levy. 2003. Clinical review: fever in intensive care unit patients. *Crit. Care.* 7:221–225.

40. Charkoudian, N. 2003. Skin blood flow in adult human thermoregulation: how it works, when it does not, and why. *Mayo Clin. Proc*. 78:603–612.

41. Hildebrandt, B., P. Wust, O. Ahlers, A. Dieing, G. Sreenivasa, T. Kerner, R. Felix, and H. Riess. 2002. The cellular and molecular basis of hyperthermia. *Crit. Rev. Oncol. Hematol*. 43:33–56.

42. Turi, A., R. C. Lu, and P. S. Lin. 1981. Effect of heat on the microtubule disassembly and its relationship to body temperatures. *Biochem. Biophys. Res. Commun*. 100:584–590.

43. Lin, P. S., D. F. Wallach, and S. Tsai. 1973. Temperature-induced variations in the surface topology of cultured lymphocytes are revealed by scanning electron microscopy. *Proc. Natl. Acad. Sci. USA*. 70: 2492–2496.

44. Lionetti, F. J., P. S. Lin, R. J. Mattaliano, S. M. Hunt, and C. R. Valeri. 1980. Temperature effects on shape and function of human granulocytes. *Exp. Hematol*. 8:304–317.

45. Shore, S. L., T. J. Romano, M. R. Hubbard, and D. S. Gordon. 1977. Lysis of virus-infected target cells by antibody-dependent cellular cytotoxicity. II. Reversibility of the heart inactivation of K cell killing and relationship of Fc receptor capping to lysis. *Cell. Immunol*. 31: 55–61.